

## Combustion, Kinetics, and Thermodynamic Characterization of Oil Palm Empty Fruit Bunch Pellets

Bemgba B. Nyakuma <sup>1</sup>, Olagoke Oladokun <sup>1,2</sup>, Tertsegba J-P. Ivase <sup>3</sup>, Aliyu Bello <sup>2</sup>, Jamila B. Ali <sup>4</sup>, Victor O. Otitolaiye <sup>5</sup>

<sup>1</sup> School of Chemical and Energy Engineering, Faculty of Engineering, Universiti Teknologi Malaysia, 81310 Skudai, Johor, Malaysia

<sup>2</sup> Department of Chemical Engineering, University of Maiduguri, P.M.B 1069, Bama Road, Maiduguri, Borno State, Nigeria

<sup>3</sup> Bio-Resource Development Centre, National Biotechnology Development Agency, Makurdi, Benue, State, Nigeria

<sup>4</sup> Department of Polymer and Textile Engineering, Ahmadu Bello University, Samaru Zaria, Kaduna State, Nigeria

<sup>5</sup> Department of Health Safety & Environmental Management, International College of Engineering & Management, Seeb, Oman

Received October 11, 2020; Accepted December 22, 2020

---

### Abstract

Combustion is considered an efficient route for the sustainable valorisation of oil palm empty fruit bunches (OPEFB) generated in Malaysia. However, OPEFB requires pre-treatment through pelletization to improve its fuel properties for combustion. Therefore, this paper seeks to examine the physicochemical, oxidative thermal (combustion), kinetic, and thermodynamic fuel properties of OPEFB pellets. Physicochemical characterisation revealed high elemental, proximate, and calorific values. Combustion characteristics revealed high thermal reactivity and conversion of the OPEFB pellets, as evident in its high mass loss ( $M_L > 92\%$ ) but low residual ash ( $R_M < 7.11\%$ ) during thermogravimetric analysis (TGA). Kinetic analysis revealed activation energies ( $E_a$ ) in the range 77.9 to 303.4 kJ/mol and frequency factor ( $A$ ) of  $2.9 \times 10^4$  to  $5.3 \times 10^{28} \text{ min}^{-1}$  based on the Flynn-Wall-Ozawa (FWO) and Kissinger-Akahira-Sunose (KAS) models. The kinetic compensation effect (KCE) was detected in the plots of  $E_a$  against  $A$  for both FWO and KAS, whereas the compensation constants  $a$ , and  $b$ , were deduced from the plots of  $\log A$  against  $E_a$ . Thermodynamic analysis revealed a high degree of disorderliness in the reactants and products, which indicate high reactivity and shorter reaction times. Therefore, the OPEFB pellets can be effectively utilised as feedstock for energy recovery through combustion.

**Keywords:** : Combustion; Biomass; Fuel Characterization; Oil Palm; Empty Fruit Bunches; Pellets.

---

## 1. Introduction

The palm oil industry is a significant contributor to socio-economic growth and sustainable development in Malaysia. According to the Agency for Innovation Malaysia (AIM), the palm oil industry (POI) accounts for 8% (RM 80 billion) of the nation's gross national income (GNI) yearly [1]. Due to its strategic economic importance, the sector has expanded exponentially over the years with increased acreage cultivation of oil palm (*Elaeis guineensis* Jacq.) for the extraction of crude palm oil (CPO). Similarly, the growing demand for CPO utilized for the production of household consumer products, biochemicals, and biodiesel has soared significantly over the years [2].

The Malaysian POI generates significant quantities of solid and liquid wastes from the cultivation of oil palm trees and extraction of CPO. It is currently estimated that the POI generates over 80 million dry tonnes of wastes comprising; oil palm fronds (OPF) and trunks (OPT),

empty fruit bunches (EFB), palm kernel shells (PKS), and palm mesocarp fibre (PMF). The enormity of the wastes currently generated by the POI has prompted calls for swift action to address the impending problems that could arise from long term accumulation and proliferation of these wastes. Consequently, stakeholders in the industry have sought to explore sustainable strategies to effectively dispose and manage the wastes, albeit with limited success. Therefore, there are growing concerns that the growing stockpiles and accumulation of oil palm wastes (OPW) could pose severe risks to human health, safety, and the environment [3].

In light of this, the government of Malaysia (GoM) promulgated the National Biomass Strategy (NBS-2020) in 2011 (revised in 2013) to explore the most socially acceptable, economic, and environmentally friendly strategies to valorise the mounting stockpiles of OPWs generated in the nation's palm oil mills. The policy aims to valorise 20%-25% or about 20 million dry tonnes of the OPW into high economic value products with the potential to contribute RM30 million to the economy by 2020. This comes against the backdrop of AIM's predictions that OPW tonnage will soar to over 100 million dry tonnes by 2020. Therefore, there is an urgent need to explore and exploit efficient strategies and technologies to reduce not only the tonnage volumes of OPW but also minimise their effects on the environment owing to long term accumulation by open dumping.

One of the most effective measures for addressing the problems of disposal and management of lignocellulosic wastes such as oil palm wastes (OPW) is through thermochemical conversion. Several studies have demonstrated the potential of various thermochemical processes such as torrefaction [4-5], liquefaction [6-8], pyrolysis [9-10], gasification [11-12], and combustion [13-14] in valorising OPW. The findings indicate that although these technologies can valorise and minimise the bulk of OPWs, the processes are hampered by numerous challenges. In addition to low conversion efficiencies, emission of pollutants, greenhouse gases (GHG) and secondary wastes, these processes are primarily hampered by the bulk nature, high alkali content, and moisture content along with low energy density, calorific values, and logistics potential of OPWs. The outlined drawbacks are particularly evident in the utilisation of oil palm empty fruit bunches (OPEFB), which is characterised by 60% moisture content, low calorific value and high alkali. Typically, these fuel properties result in low conversion efficiencies, low product yield, tar formation and distribution along with operational challenges such as agglomeration, sintering, and equipment fouling [11, 15-16]. Consequently, OPEFB requires extensive pre-treatment and conditioning through drying, bulk reduction and densification to improve its fuel properties, energy recovery potential and suitability for thermochemical conversion through combustion [17].

Combustion is one of the oldest technologies for energy recovery from carbonaceous materials such as biomass. It is an exothermic process that involves the oxidative conversion of carbonaceous materials into water, carbon dioxide, and heat at high temperatures [18-19]. The production of heat in combustion reactors (boilers) is a primary process in the palm oil mills for the production of steam used to strip, sterilise, and wash fresh fruit bunches. Currently, OPMs in Malaysia utilise OPWs such as OPEFB in boilers, albeit inefficiently, for steam production. The low efficiency is due to the poor fuel properties of OPEFB, which accounts for 23% or (23%) of all OPWs generated in the palm oil mills. However, it is envisaged that the pre-treatment of OPEFB through drying, mechanical disintegration, and pelletization will improve its fuel properties for effective utilisation as boiler fuel. However, there are limited studies on the combustion of OPEFB pellets in literature. Some researchers have examined OPEFB pellets pyrolysis [20-21], and gasification [22-25]. The findings revealed operational challenges such as poor ignition, low gas yields and product distribution, tar formation and high energy requirements. Other studies have shown that the combustion of pulverised EFB results in ash formation and deposition [26-28], greenhouse gas and pollutant emissions, and low reactivity (high activation energies) [29], which are ascribed to the poor fuel properties pulverised OPEFB. Therefore, it is imperative to comprehensively characterise the fuel properties of OPEFB pellets to examine its physicochemical and thermal characteristics for application in future combustion systems.

Based on the challenges outlined, this study seeks to examine the oxidative (combustion) thermal, kinetic degradation, and thermodynamic properties of oil palm empty fruit bunches (OPEFB) pellets through thermogravimetric analysis (TGA). It also seeks to characterise, examine, and highlight the physicochemical fuel properties of the OPEFB pellets as a potential feedstock for combustion. The findings will present significant insights into thermal degradation behaviour, temperature profile characteristics, and potential reaction pathway for OPEFB pellet combustion.

## 2. Materials and methods

### 2.1. Materials

The oil palm empty fruit bunch pellets (or OPEFB Pellets) were obtained from an oil palm mill in Kota Tinggi in the state of Johor (Malaysia). The OPEFB Pellets were subsequently transported to the Hydrogen and Fuel Cell Laboratory, Universiti Teknologi Malaysia for further analysis. The brown, uniformly shaped, and cylindrical 8 mm diameter OPEFB Pellets each weigh 2.5 g. Before characterisation, the OPEFB Pellets were pulverised in a high-speed crusher (Model: Panasonic Super Mixer Grinder MX-AC400, Malaysia). The pulverised sample was subsequently sieved using a standard laboratory analysis sieve of mesh size 60 (250  $\mu\text{m}$  or 0.0098 inches) (Brand: W.S. Tyler, Mexico) to obtain homogenous sized particles. Next, the OPEFB Pellets were subjected to extensive characterisation to determine its physicochemical, thermal, kinetic, and thermodynamic fuel properties.

### 2.2. Physicochemical analysis

The elemental analysis of the OPEFB pellets was examined based on the ASTM standard D5291-10 (2015) for determining the elemental (CHNS–Carbon, Hydrogen, Nitrogen, and Sulphur, respectively) composition of fuels. For each test, 5 mg of pulverised OPEFB pellets were weighed, wrapped in a tin foil capsule, and placed in the autosampler of the CHNS analyser (Model: vario MICRO cube *Elementar Analysensysteme* GmbH, Germany). Next, the elemental carbon (C), hydrogen (H), nitrogen (N) and sulphur (S) in the sample were converted into  $\text{CO}_2$ ,  $\text{H}_2\text{O}$ ,  $\text{NO}_2$  and  $\text{SO}_2$ , respectively through excess oxygen combustion in the bomb calorimeter at 1150°C. The evolved gases were subsequently detected using the TCD and quantified using column chromatography (CC) to detect the percentage elemental composition of CHNS in the sample. The proximate analysis was determined by the ASTM standards; D3173-87 (2003) for moisture content (MC), D3175-07 (2007) for volatile matter (VM) and D3174-04 (2004) for ash content (AC) in a muffle furnace (Model; NeyTech Vulcan D-130, USA). Lastly, the calorific analysis was performed using the isoperibol oxygen bomb calorimeter (Model: IKA C2000, USA) to determine the higher heating value (HHV) according to the ASTM standard D-2015. Each test was repeated at least three times to ensure the reliability and accuracy of the measurements and the results presented, as average values in Table 1.

### 2.3. Thermal analysis

The oxidative thermal analysis of OPEFB pellets was performed by thermogravimetric analysis (TGA). The TGA runs were performed on the Shimadzu Thermogravimetric Analyser (Model: TGA-50, Japan). For each run, about 10 mg of sample was placed in an alumina crucible and transferred to the sample bucket of the TG analyser. Next, the sample was heated under non-isothermal conditions from 30 °C to 800 °C at different heating rates from 5, 10, 15, 20 and 30°C/min. During the TG analysis, air was used as the purge gas and to simulate the oxidative environment for combustion at a flow rate of 20 ml/min. On completion, the raw TG data were retrieved and analysed using the Shimadzu Thermal Analysis (STA) software (Version: TA-60WS Workstation) to deduce the mass loss (TG/DTG) data and characteristic temperature profiles (TPC) for further analysis. Consequently, Microsoft Excel (version 2013) was used to plot the mass loss (%) and derivative mass loss (%) data against temperature (°C) to obtain thermogravimetric (TG, %) and derivative thermogravimetric (DTG, %/min) plots, respectively. Based on the plots, the TPCs determined using the STA

software included; onset (ignition) ( $T_{onset}$ ), peak decomposition ( $T_{peak}$ ), offset (burnout) ( $T_{end}$ ), and midpoint ( $T_{mid}$ ) temperatures. Furthermore, the mass loss ( $M_L$ ), and residual mass ( $R_M$ ) were estimated to examine the thermal degradation behaviour, conversion and reactivity of the OPEFB pellets.

## 2.4. Kinetic analysis

This analysis was performed to determine the kinetic parameters for the oxidative thermal decomposition of the OPEFB Pellets. This was accomplished by applying the multi-heating rate, non-isothermal thermogravimetric analysis (TGA) data to the isoconversional kinetic models of Flynn-Wall-Ozawa (FWO) and Kissinger-Akahira-Sunose (KAS). The models are based on the one-step global model for the thermal decomposition of carbonaceous materials. According to the model, biomass decomposition occurs via a single reaction pathway expressed as [30]:



Based on the model, the degree of conversion ( $\alpha$ ) for biomass at temperature ( $T$ , K) and time ( $t$ , in seconds) is represented by the relation:

$$\alpha = \frac{m_i - m_a}{m_i - m_f} \quad (2)$$

The terms  $m_i$ ,  $m_a$ , and  $m_f$  denote the initial, actual, and final masses of the thermally decomposing OPEFB Pellets in which the temperature dependency is described by Arrhenius equation:

$$k = A \exp\left(\frac{-E_a}{RT}\right) \quad (3)$$

The term  $k$  represents the rate constant,  $A$  - pre-exponential factor ( $\text{min}^{-1}$ ),  $E_a$  - activation energy (kJ/mol),  $R$  - molar gas constant (J/mol K), and  $T$  - absolute temperature (K). Hence, the rate of thermal decomposition of the sample can now be expressed as:

$$\frac{d\alpha}{dt} = k(T)f(\alpha) \quad (4)$$

where  $f(\alpha)$  is the reaction model for OPEFB Pellet decomposition during thermal analysis. For a given order of reaction,  $n$ , the reaction model is defined:

$$f(\alpha) = (1 - \alpha)^n \quad (5)$$

Therefore, the multi-heating rate ( $\beta$ ) decomposition of biomass can be deduced from the integral of relation [31]:

$$\frac{d\alpha}{(1 - \alpha)^n} = \frac{A}{\beta} \exp\left(\frac{-E_a}{RT}\right) dT \quad (6)$$

The integral solution of the equation is the basis for the FWO and KAS models used to determine the kinetic parameters activation energy,  $E_a$  and frequency factor,  $A$ , of thermally decomposing materials. Therefore, the kinetic analyses of OPEFB pellets decomposition under oxidative conditions was examined based on the corresponding temperatures ( $T$ , K) for each conversion ( $\alpha$ ) as determined from the mass loss (TG, %) data. The values were consequently applied to the governing equations of the Flynn-Wall-Ozawa (FWO) and Kissinger-Akahira-Sunose (KAS) models described in subsequent sections of this paper.

### 2.4.1. Flynn-Wall-Ozawa

The kinetic parameters for OPEFB Pellets decomposition under the oxidative conditions were examined based on the Flynn-Wall-Ozawa (FWO) model. This was realised by plotting  $\ln(\beta)$  against  $1000/T$  for the degree of conversions  $\alpha = 0.10$  to  $0.70$  as described in the equation:

$$\ln(\beta) = \ln\left(\frac{AE_a}{Rg(\alpha)}\right) - 5.331 - 1.052\left(\frac{-E_a}{RT}\right) \quad (7)$$

Next, the activation energy,  $E_a$  and frequency factor,  $A$  were calculated from the slope [ $-1.052 E_a/R$ ] and intercept [ $\ln(AE_a/R)$ ], respectively.

### 2.4.2. Kissinger-Akahira-Sunose

The Kissinger-Akahira-Sunose (KAS) model was also used to compute the kinetic parameters for OPEFB pellets decomposition under oxidative conditions. Hence, the term  $\ln(\beta/T_2)$  was plotted against  $1000/T$  for the conversions of  $\alpha = 0.10$  to  $0.70$  as described in the equation:

$$\ln\left(\frac{\beta}{T^2}\right) = \ln\left(\frac{AR}{g(\alpha)E_a}\right) - \left(\frac{-E_a}{RT}\right) \quad (8)$$

Consequently, the activation energy,  $E_a$  and frequency factor,  $A$  were computed from the slope  $-E_a/R$  and intercept  $[\ln(AR/E_a)]$  of the plots, respectively.

### 2.5. Thermodynamic analysis

The thermodynamic parameters; enthalpy ( $\Delta H$ ), Gibb's free energy ( $\Delta G$ ), and entropy change ( $\Delta S$ ) for the OPEFB pellets were computed from the  $E_a$  and  $A$  of the FWO model and DTG peak temperature ( $T_{peak} = 302.20^\circ\text{C}$  or  $575.35\text{K}$ ) at  $5^\circ\text{C}/\text{min}$ . The terms  $\Delta H$ ,  $\Delta G$ , and  $\Delta S$  were calculated from the equations [32];

$$\Delta H = E_a - RT \quad (9)$$

$$\Delta G = E_a + RT_{peak} \ln\left(\frac{K_B T_{peak}}{hA}\right) \quad (10)$$

$$\Delta S = \frac{\Delta H - \Delta G}{T_{peak}} \quad (11)$$

The terms;  $\Delta H$  represent the enthalpy (kJ/mol);  $\Delta G$  - Gibb's free energy (kJ/mol);  $\Delta S$  - entropy change (J/mol);  $T_{peak}$  - peak decomposition temperature ( $^\circ\text{C}$ );  $K_B$  - Boltzmann's constant ( $1.38 \times 10^{-23}$ , J/K); and  $h$  - Planck's constant ( $6.626 \times 10^{-34}$ , Js).

## 3. Results and discussion

### 3.1. Physicochemical properties

Table 1 presents the elemental, proximate, and calorific fuel properties of the OPEFB pellets examined in this study. All the fuel properties are averaged values from three determinations presented in as received (ar) basis.

Table 1. Physicochemical fuel properties of OPEFB pellets

Element/Property	Symbol	Units	Composition
Carbon	C	(wt.%)	41.71
Hydrogen	H	(wt.%)	5.53
Nitrogen	N	(wt.%)	1.12
Sulphur	S	(wt.%)	0.12
Oxygen	O	(wt.%)	51.53
Moisture	MC	(wt.%)	7.78
Volatile matter	VM	(wt.%)	75.19
Ash	A	(wt.%)	5.80
Fixed carbon	FC	(wt.%)	11.24
High Heating Value	HHV	(MJ/kg)	17.57

As observed, OPEFB pellets contain a high composition of  $C$ ,  $H$ , and  $O$  but low  $N$  and  $S$ . The high  $C$ ,  $H$ , and  $O$  accounts for the reactivity and calorific value of oil palm biomass [33]. Furthermore, the low  $N$  and  $S$  composition indicates the fuel has a low potential for  $\text{SO}_x$  and  $\text{NO}_x$  emissions, which makes it a potentially environmentally friendly feedstock for thermal conversion. Overall, the pellet properties are in good agreement with other biomass typically in the range  $C = 42\text{--}71$  wt.%,  $H = 3\text{--}11$  wt.%,  $N = 0.1\text{--}12$  wt.%,  $S = 0.01\text{--}2.3$  wt.% and  $O = 16\text{--}49$  wt.% [34]. The proximate analysis revealed high volatile matter ( $VM$ ) and fixed carbon ( $FC$ ) along with low moisture ( $MC$ ) and ash ( $A$ ) content. Similarly, the results are in good agreement with other biomass typically in the range  $MC = 3\text{--}63$  wt. %;  $VM = 48\text{--}86$  wt. %;  $A = 0.1\text{--}45$  wt. %, and  $FC = 1\text{--}38$  wt. % [34]. The  $VM$  indicates the high condensable and non-condensable gases, whereas the high  $FC$  indicates the thermal conversion of OPEFB

pellets could yield high gas products. The low  $MC < 10\%$  and AC indicate high conversion efficiency, lower energy input, and operating costs for thermal conversion of the OPEFB pellets [35]. Lastly, the higher heating value (HHV) of OPEFB pellets is 17.57 MJ/kg, which is in good agreement with reported values (14 – 22 MJ/kg) for other biomass in the literature [36].

### 3.2. Thermal properties

The thermal degradation behaviour and temperature profile characteristics of OPEFB pellets were examined by TGA, as presented in TG and DTG plots in Figures 1 and 2, respectively. The resulting plots showed that the oxidative thermal degradation of OPEFB pellets resulted in progressive mass loss. This is evident in the “double Z” downward sloping curves observed during TGA. This observation demonstrates that the increase in temperature and heating rates significantly influenced the thermal degradation of OPEFB pellets during TGA. This is evident in the shift in the TG plots to the right-hand side of Figures 1 and 2 as the heating rates increased from 5 °C/min to 30 °C/min. As a result of the shifts, the temperature profile characteristics (TPC) were also transformed accordingly. The changes in the TPC; onset (ignition) ( $T_{onset}$ ) and offset (burnout) ( $T_{end}$ ) temperatures, along with the mass loss ( $M_L$ ), and residual mass ( $R_M$ ) during oxidative TGA were deduced, as presented in Table 2.

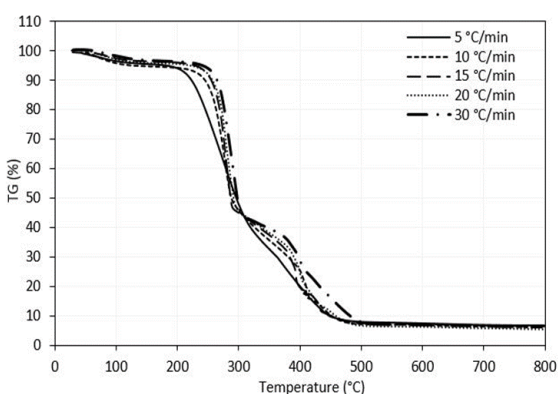


Figure 1. TG plots for oxidative thermal degradation of OPEFB pellets

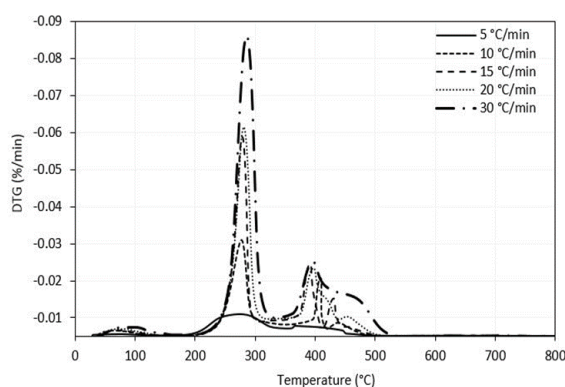


Figure 2. DTG plots for oxidative thermal degradation of OPEFB pellets

Table 2. Combustion characteristics of OPEFB pellets

Heating rate (°C/min)	Onset ( $T_{onset}$ , °C)	Offset ( $T_{end}$ , °C)	Mass loss ( $M_L$ , %)	Residual mass ( $R_M$ , %)
5	219.00	367.56	92.89	7.11
10	249.03	318.14	94.14	5.86
15	257.60	313.24	93.73	6.27
20	262.01	327.97	94.90	5.10
30	260.57	337.05	93.97	6.03

As observed, the increase in the heating rates from 5 °C/min to 30 °C/min changed the TPC accordingly. Hence, the ignition temperature ( $T_{onset}$ ) of the fuel increased from 219°C to 262.01°C, whereas the burnout temperature ( $T_{end}$ ) was from 313°C to 367.56°C. On average, the average ignition temperature ( $T_{onset}$ ) was 249.64 °C, whereas the burnout temperature ( $T_{end}$ ) was 332.79°C. The results indicate that the devolatilization of OPEFB pellets occurred primarily between 220 °C and 368 °C based on the conditions examined in this study. Next, the mass loss ( $M_L$ ), and residual mass ( $R_M$ ) of the process was examined to examine the thermal degradation behaviour and potential ash yield from OPEFB pellet degradation. As observed in Table 2, the  $M_L$  increased from 92.89 % to 94.90 %, whereas  $R_M$  was between 5.10 % and 7.11 %. This finding indicates the oxidative degradation process resulted in 93.92 % mass loss and 6.08 % residues or ash, on average. In comparison, the ash content of the fuel from the proximate analysis was 5.80% (Table 1), which is in good agreement with the

$R_M$  of the OPEFB pellets during the oxidative TGA process. The results demonstrate that combustion of the pellets may not pose significant problems such as ash sintering, agglomeration or fouling during thermochemical conversion in a future combustor. However, this is expedient on performing ash characterisation analyses, which is beyond the scope of this study.

Based on the size, symmetry and position of the peaks, the oxidative thermal decomposition process occurred in four (4) stages namely: Stage I (30–200)°C, Stage II (200–325)°C, Stage III (325–525) °C and finally, Stage IV (525–800)°C. Stage I is characterised by the peaks between 30°C and 200°C. The mass loss during this stage is ascribed to loss of moisture and low molecular weight volatiles. Stage II, on the other hand, is attributed to the decomposition of volatile matter into char and other intermediate products. The size of the peaks indicates the process is highly reactive, resulting in significant char or carbon formation. Stage III is due to the combustion of char (formed in stage II) into ash, mineral matter and other products. This stage of the process appears to be also highly reactive due to numerous smaller peaks from 350–550°C observed at each heating rate. This observation suggests there may also be simultaneous or parallel formation and decomposition of char and other intermediates into ash and other products occurring during the oxidative process. Lastly, stage IV is characterised by the tailing observed after 550°C, as also detected in the TG plots. This process is due to the decomposition of residual char and intermediate products in the residual ash. In summary, the processes occurring during the oxidative degradation of the OPEFB pellets can be summarised as; Stage I – drying, Stage II – devolatilization, Stage III – char conversion and lastly, Stage IV – ash formation. Next, the effect of heating rates on the DTG plots was examined. Similarly, the increase in heating rates from 5°C/min to 30°C/min also significantly influenced the mass loss rate ( $M_L$ ) rate and peak decomposition temperatures ( $T_{peak}$ ) for drying and devolatilization, as presented in Table 3.

Table 3. DTG peak temperatures for OPEFB pellets combustion

Stage Heating rate (°C/min)	Drying (30 – 200 °C)		Devolatilization (200 – 325 °C)	
	Drying temp (°C)	$M_L$ Rate (%/Min)	$T_{peak}$ (°C)	$M_L$ Rate (%/min)
5	75.76	0.15	272.93	3.04
10	69.66	0.78	276.78	13.41
15	80.01	0.63	277.17	27.80
20	84.79	0.77	282.00	31.83
30	98.13	1.05	286.46	42.60

The results revealed that the drying process occurred between 69.66°C and 98.13°C with increasing heating rates. Conversely, devolatilization occurred between 272.93°C and 286.46°C. During the process, the  $M_L$  rate for drying increased from 0.15 %/min to 1.05 %/min compared to 3.04 %/min to 42.60 %/min observed for devolatilization. This confirms that the devolatilization process is the most reactive and temperature-dependent stage of the multi-heating rate combustion of the OPEFB pellets. However, the reactivity of the oxidative process and temperature dependency of the process is best examined through kinetic analyses. Therefore, the kinetic analysis was performed to determine the oxidative degradation parameters for the OPEFB pellets by applying the TG data to the *isoconversional* kinetic models of Flynn-Wall-Ozawa (FWO) and Kissinger-Akahira-Sunose (KAS).

### 3.3. Kinetic properties

The kinetic parameters namely; activation energy ( $E_a$ , kJ/mol) and frequency factor ( $A$ , min<sup>-1</sup>) were deduced at degrees of conversions:  $\alpha = 0.10$  to 0.70 after applying the plots of FWO and KAS kinetic models presented in Figures 3 and 4.

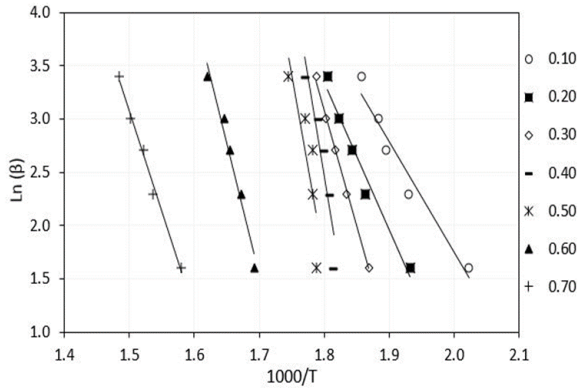


Figure 3. FWO kinetic plots for the oxidative thermal degradation of OPEFB pellets

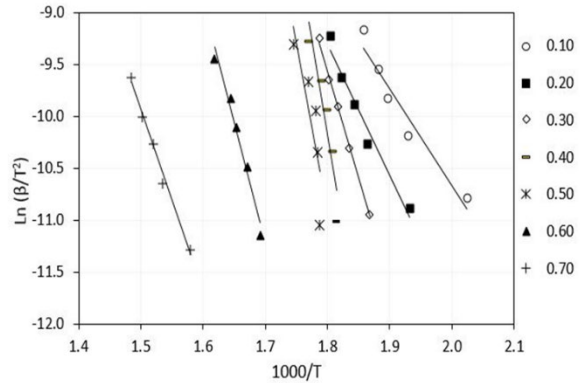


Figure 4. KAS kinetic plots for the oxidative thermal degradation of OPEFB pellets

As observed, the FWO and KAS kinetic plots for the oxidative thermal degradation of the OPEFB Pellets appear as sets of various distinguishable parallel lines. According to Miura and Maki [37], the parallel arrangement of kinetic line plots signifies the various stages thermally decomposing materials undergo during TGA. Therefore, the oxidative thermal degradation of the OPEFB pellets can be described in four (4) stages:  $\alpha = 0.0 - 0.30$ ;  $\alpha = 0.40 - 0.05$ ;  $\alpha = 0.60$  and  $\alpha = 0.70$ . This validates the earlier submission that the oxidative thermal degradation of the pellets occurs in four stages corresponding to drying (Stage I), devolatilization (Stage II), char conversion (Stage III) and ash formation (Stage IV).

Next, the kinetic parameters  $E_a$  and  $A$  were calculated from the slope and intercept of the FWO and KAS kinetic plots in Figures 3 and 4, respectively. The calculated  $E_a$  and  $A$  for the oxidative thermal decomposition of the OPEFB Pellets are presented in Table 4.

Table 4. Kinetic parameters for OPEFB pellet combustion

Conversion $\alpha$	FWO Model			KAS Model		
	$R^2$	$E_a$ (kJ/mol)	$A$ ( $\text{min}^{-1}$ )	$R^2$	$E_a$ (kJ/mol)	$A$ ( $\text{min}^{-1}$ )
0.10	0.9574	82.14	$6.23 \times 10^8$	0.9486	77.86	$2.94 \times 10^4$
0.20	0.9747	109.21	$1.37 \times 10^{11}$	0.9706	106.00	$1.08 \times 10^7$
0.30	0.9975	170.90	$8.48 \times 10^{16}$	0.9973	170.69	$1.62 \times 10^{13}$
0.40	0.8900	295.30	$5.34 \times 10^{28}$	0.8838	303.36	$3.01 \times 10^{25}$
0.50	0.7247	272.60	$1.53 \times 10^{26}$	0.7111	277.36	$7.07 \times 10^{22}$
0.60	0.9711	194.04	$2.66 \times 10^{17}$	0.9680	194.08	$5.37 \times 10^{13}$
0.70	0.9915	148.85	$2.25 \times 10^{12}$	0.9903	145.74	$2.24 \times 10^8$
Average	0.9296	181.86	$7.65 \times 10^{27}$	0.9242	182.16	$4.31 \times 10^{24}$

The results for the FWO model indicate that the  $E_a$  ranged from 82.14 kJ/mol to 295.30 kJ/mol with an average of 181.86 kJ/mol, whereas  $A$  was from  $6.23 \times 10^8 \text{ min}^{-1}$  to  $5.34 \times 10^{28} \text{ min}^{-1}$  with an average value of  $7.65 \times 10^{27} \text{ min}^{-1}$  at  $R^2 = 0.93$  on average. As observed, the kinetic parameters increased gradually from 82.14 kJ/mol with a peak value of 295.30 kJ/mol before dropping to 148.85 kJ/mol. This indicates the reactivity decreased during conversion but slowed considerably at  $\alpha = 0.40$  (with  $E_a = 295.30 \text{ kJ/mol}$ ), indicating this is the rate-limiting step of the process. Based on the earlier submission, the decomposition at  $\alpha = 0.40$  falls into Stage II or the devolatilization stage of the process. In contrast, the kinetic parameters  $E_a$  for the KAS model ranged from 77.86 kJ/mol to 303.36 kJ/mol with an average value of 182.16 kJ/mol, whereas  $A$  was from  $2.94 \times 10^4 \text{ min}^{-1}$  to  $3.01 \times 10^{25} \text{ min}^{-1}$  with an average of  $4.31 \times 10^{24} \text{ min}^{-1}$ . The average  $R^2$  value for FWO was 0.92. Similarly, the model's kinetic parameters increased gradually from 77.86 kJ/mol, peaked at 303.36 kJ/mol before falling to 145.74 kJ/mol. Therefore, the parameters for the model increased but slowed considerably at  $\alpha = 0.40$ , as also observed for the FWO model. Therefore, the rate-limiting step for the model occurs at 40% conversion. Overall, the results demonstrate that the FWO and KAS models

successfully described the oxidative thermal degradation of OPEFB pellets. Furthermore, the results revealed the kinetic parameters;  $E_a$  and  $A$  for the oxidative decomposition of the OPEFB pellets fluctuated between 77.86 kJ/mol and 303.36 kJ/mol and from  $2.94 \times 10^{04}$  to  $5.34 \times 10^{28}$   $\text{min}^{-1}$ , respectively. To examine the extent of variability between the kinetic parameters typically described as the kinetic compensation effect (KCE), the relationship between the  $E_a$ , and  $A$  for the oxidative degradation of OPEFB Pellets was examined, as presented in Figures 5 and 6.

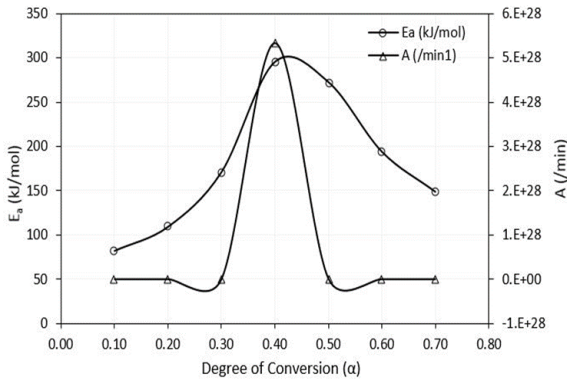


Figure 5. KCE plots for FWO model

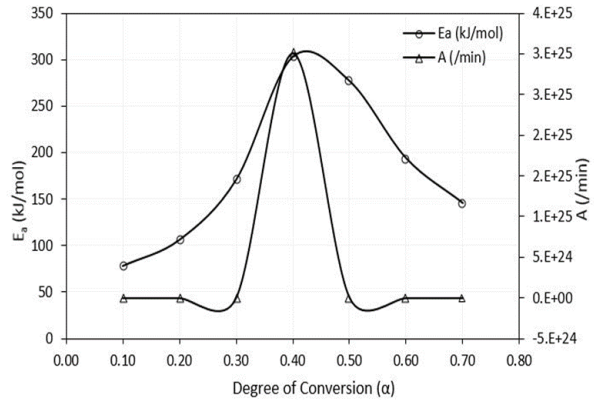


Figure 6. KCE plots for KAS model

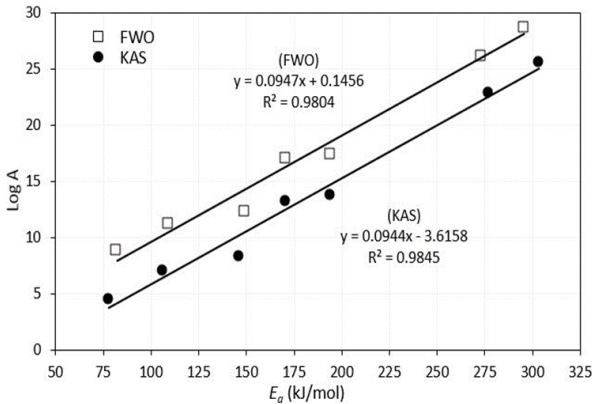


Figure 7. KCE plots of Log A against  $E_a$  for OPEFB Pellets Degradation

As observed in the FWO and KAS plots reveal that the activation energy ( $E_a$ ) increased concurrently with the frequency factor ( $A$ ) as defined by the theory of the kinetic compensation effect (KCE). The results demonstrate that irrespective of the selected model, the effect of kinetic compensation occurred during thermal conversion of the OPEFB pellets. In addition, the highest  $E_a$  and  $A$  values occurred at 40% conversion ( $\alpha = 0.40$ ), which confirms it is the rate-limiting step. Based on the Zsako [38] relation, the compensation constants  $a$  and  $b$  for OPEFB pellets were deduced from the plots of Log A against  $E_a$  in Figure 7.

The results demonstrate there is a correlation between the natural logarithm of frequency factor ( $A$ ) and the activation energy ( $E_a$ ) for the oxidative TG decomposition of the OPEFB pellets. Based on the plots, the compensation constants for the FWO model are  $a = 0.095$  and  $b = 0.15$  with an  $R^2$  of 0.98. However, the values for KAS are  $a = 0.094$  and  $b = -3.62$  with an  $R^2$  of 0.98.

### 3.4. Thermodynamic properties

The thermodynamic parameters; enthalpy ( $\Delta H$ ), Gibb's free energy ( $\Delta G$ ) and entropy change ( $\Delta S$ ) for OPEFB pellets degradation were also examined based on the procedure in the literature [32]. Similarly, the kinetic parameters  $E_a$  and  $A$  deduced from the Flynn-Wall-Ozawa (FWO) model and peak decomposition temperature  $T_{peak} = 272.93^\circ\text{C}$  (or 546.08 K) at  $5^\circ\text{C}/\text{min}$  were adopted for the parametric calculations. The calculated values for  $\Delta H$ ,  $\Delta G$ , and  $\Delta S$  for the oxidative thermal decomposition of the OPEFB pellets are presented in Table 5.

Table 5. Oxidative thermodynamic properties

Conversion ( $\alpha$ )	$\Delta H$ (kJ/mol)	$\Delta G$ (kJ/mol)	$\Delta S$ (J/mol)
0.10	78.03	310.57	-232.53
0.20	104.91	362.11	-257.21
0.30	166.45	484.36	-317.91
0.40	290.72	732.11	-441.39
0.50	267.95	682.83	-414.89
0.60	189.12	512.69	-323.57
0.70	143.58	414.46	-270.88
Average	177.25	499.88	-322.62

As observed, the  $\Delta S$  fluctuated from -441.39 J/mol to -232.53 J/mol, whereas the  $\Delta H$  was between 78.03 kJ/mol to 290.72 kJ/mol; and lastly, the  $\Delta G$  was from 310.57 kJ/mol to 732.11 kJ/mol. Therefore, the average thermodynamic values deduced are; enthalpy ( $\Delta H = 177.25$  kJ/mol), Gibb's free energy ( $\Delta G = 499.88$  kJ/mol) and entropy change ( $\Delta S = -322.62$  J/mol). Typically, the negative entropy ( $\Delta S$ ) values indicate that the degree of disorderliness of the initial reactants is higher than the products formed through the dissociation of bonds during the oxidative thermal degradation process [32]. However, the high entropy values indicate higher reactivity and shorter time to attain the activated complex and hence, the shorter overall time of reaction [39]. The values of Gibb's free energy, on the other hand, showed that the total increase in energy of the system along with the formation of the activated complex is high for the oxidative thermal degradation of OPEFB pellets [40-41]. This accounts for the high mass loss ( $M_L = 92.9$  to  $94.9\%$ ) and low yield of residuals (ash) observed for the OPEFB pellets, earlier presented in Table 2.

#### 4. Conclusion

The paper presented the combustion kinetics and thermodynamic characteristics of oil palm empty fruit bunches (OPEFB) pellets. The fuel characterisation of the OPEFB pellets showed a high composition of elemental, proximate, and calorific content for efficient energy recovery through thermal conversion processes such as combustion. Consequently, the combustion characteristics were examined through oxidative thermal analysis, which showed that OPEFB pellets are highly reactive with high mass loss ( $M_L = 92.9$ – $94.9\%$ ), mass loss rates ( $M_{LR} = 3.0$ – $42.6$  %/min) along with low residual mass or ash yields ( $R_M = 5.10$ – $7.11\%$ ). The kinetic analysis revealed that the oxidative thermal degradation of OPEFB pellets is also highly reactive with kinetic parameters; activation energy ( $E_a$ ) ranging from 77.86 to 303.36 kJ/mol and frequency factor ( $A$ ) from  $2.94 \times 10^4$  to  $5.34 \times 10^{28}$  min<sup>-1</sup> based on the isoconversional kinetic models of Flynn-Wall-Ozawa (FWO) and Kissinger-Akahira-Sunose (KAS). Lastly, the thermodynamic analysis revealed that the degree of disorderliness of the products formed through the dissociation of bonds is lower than the initial reactants during the oxidative degradation process. The high entropy values recorded for the pellets indicate high reactivity, which could result in shorter times and overall reaction times for the formation of an activated complex. In conclusion, the OPEFB pellet is a potentially practical feedstock for efficient energy recovery through oxidative (combustion) thermal degradation.

#### Acknowledgements

The material assistance of the Universiti Teknologi Malaysia (UTM), Skudai Johor Bahru (Malaysia) is gratefully acknowledged. Further, the technical support of Hydrogen and Fuel Cell Laboratory, School of Chemical and Energy Engineering (UTM) towards the thermogravimetric analysis (TGA) is worthy of mention.

**References**

- [1] AIM, National Biomass Strategy 2020. 2013; Agensi Inovasi Malaysia (AIM), : Kuala Lumpur, Malaysia. 1-40.
- [2] Johari, A, Nyakuma, BB, Nor, SHM, Mat, R, Hashim, H, Ahmad, A, Zakaria, ZY, and Abdullah, TAT. The challenges and prospects of palm oil based biodiesel in Malaysia. *Energy*, 2015; 81: 255-261.
- [3] Nyakuma, BB, Wong, S, and Oladokun, O. Non-oxidative thermal decomposition of oil palm empty fruit bunch pellets: fuel characterisation, thermogravimetric, kinetic, and thermodynamic analyses. *Biomass Conversion and Biorefinery*, 2019: <https://doi.org/10.1007/s13399-019-00568-1>.
- [4] Uemura, Y, Omar, W, Othman, NA, Yusup, S, and Tsutsui, T. Torrefaction of oil palm EFB in the presence of oxygen. *Fuel*, 2013; 103: 156-160.
- [5] Uemura, Y, Omar, WN, Tsutsui, T, and Yusup, SB. Torrefaction of oil palm wastes. *Fuel*, 2011; 90(8): 2585-2591.
- [6] Akhtar, J, Kuang, SK, and Amin, NS. Liquefaction of empty palm fruit bunch (EPFB) in alkaline hot compressed water. *Renewable Energy*, 2010; 35(6): 1220-1227.
- [7] Pua, FL, Zakaria, S, Chia, CH, Fan, SP, Rosenau, T, Potthast, A, and Liebner, F. Solvolytic Liquefaction of Oil Palm Empty Fruit Bunch (EFB) Fibres: Analysis of Product Fractions Using FTIR and Pyrolysis-GCMS. *Sains Malaysiana*, 2013; 42(6): 793-799.
- [8] Yim, SC, Quitain, AT, Yusup, S, Sasaki, M, Uemura, Y, and Kida, T. Metal oxide-catalyzed hydrothermal liquefaction of Malaysian oil palm biomass to bio-oil under supercritical condition. *Journal of Supercritical Fluids*, 2017; 120: 384-394.
- [9] Abdullah, N and Sulaiman, F, The Oil Palm Wastes in Malaysia, in *Biomass Now-Sustainable Growth and Use*. 2013; InTech Open Publishers. p. 75-93.
- [10] Kabir, G and Hameed, B. Recent progress on catalytic pyrolysis of lignocellulosic biomass to high-grade bio-oil and bio-chemicals. *Renewable and Sustainable Energy Reviews*, 2017; 70: 945-967.
- [11] Samiran, NA, Jaafar, MNM, Ng, J-H, Lam, SS, and Chong, CT. Progress in biomass gasification technique-With focus on Malaysian palm biomass for syngas production. *Renewable and Sustainable Energy Reviews*, 2016; 62: 1047-1062.
- [12] Nyakuma, BB, Ahmad, A, Johari, A, Abdullah, TA, Oladokun, O, and Alkali, H. Fluidised Bed Gasification and Chemical Exergy Analysis of Pelletised Oil Palm Empty Fruit Bunches. *Chemical Engineering Transactions*, 2017; 56(1): 1159-1164.
- [13] Faizal, H, Latiff, Z, Wahid, MA, and Darus, A. Physical and combustion characteristics of biomass residues from palm oil mills. *New aspects of fluid mechanics, heat transfer and environment*, 2010: 34-38.
- [14] Lee, T, Zubir, ZA, Jamil, FM, Matsumoto, A, and Yeoh, FY. Combustion and pyrolysis of activated carbon fibre from oil palm empty fruit bunch fibre assisted through chemical activation with acid treatment. *Journal of Analytical and Applied Pyrolysis*, 2014; 110: 408-418.
- [15] Lahijani, P and Zainal, ZA. Fluidized Bed Gasification of Palm Empty Fruit Bunch Using Various Bed Materials. *Energy Sources Part A: Recovery, Utilization, and Environmental Effects*, 2014; 36(22): 2502-2510.
- [16] Sukiran, MA, Abnisa, F, Daud, WMAW, Bakar, NA, and Loh, SK. A review of torrefaction of oil palm solid wastes for biofuel production. *Energy Conversion and Management*, 2017; 149: 101-120.
- [17] Nyakuma, BB, Ahmad, A, Johari, A, Tuan, TA, Oladokun, O, and Aminu, DY. Non-Isothermal Kinetic Analysis of Oil Palm Empty Fruit Bunch Pellets by Thermogravimetric Analysis. *Chemical Engineering Transactions*, 2015; 45: 1327-1332.
- [18] McKendry, P. Energy production from biomass (part 2): conversion technologies. *Bioresource Technology*, 2002; 83(1): 47-54.
- [19] Basu, P. *Combustion and Gasification in Fluidized Beds*. 2006.
- [20] Salema, AA and Ani, FN. Pyrolysis of oil palm empty fruit bunch biomass pellets using multi-mode microwave irradiation. *Bioresource Technology*, 2012; 125: 102-107.
- [21] Lam, PS, Lam, PY, Sokhansanj, S, Lim, CJ, Bi, XT, Stephen, JD, Pribowo, A, and Mabee, WE. Steam explosion of oil palm residues for the production of durable pellets. *Applied Energy*, 2015; 141: 160-166.
- [22] Erlich, C, Öhman, M, Björnbom, E, and Fransson, TH. Thermochemical characteristics of sugar cane bagasse pellets. *Fuel*, 2005; 84(5): 569-575.

- [23] Nyakuma, BB, Mazangi, M, Tuan Abdullah, TA, Johari, A, Ahmad, A, and Oladokun, O. Gasification of Empty Fruit Bunch Briquettes in a Fixed Bed Tubular Reactor for Hydrogen Production. *Applied Mechanics and Materials*, 2014; 699: 534-539.
- [24] Erlich, C and Fransson, TH. Downdraft gasification of pellets made of wood, palm-oil residues respective bagasse: Experimental study. *Applied Energy*, 2011; 88(3): 899-908.
- [25] Nyakuma, BB, Ahmad, A, Johari, A, Abdullah, TAT, Oladokun, O, and Alkali, H. Gasification of Oil Palm Empty Fruit Bunches (OPEFB) Briquettes for Bio-Syngas Production. *Jurnal Teknologi*, 2016; 78(8-3): 83-88.
- [26] Konsomboon, S, Pipatmanomai, S, Madhiyanon, T, and Tia, S. Effect of kaolin addition on ash characteristics of palm empty fruit bunch (EFB) upon combustion. *Applied Energy*, 2011; 88(1): 298-305.
- [27] Madhiyanon, T, Sathitruangsak, P, Sungworagarn, S, Pipatmanomai, S, and Tia, S. A pilot-scale investigation of ash and deposition formation during oil-palm empty-fruit-bunch (EFB) combustion. *Fuel processing technology*, 2012; 96: 250-264.
- [28] Chin, KL, H'ng, PS, Paridah, MT, Szymona, K, Maminski, M, Lee, SH, Lum, WC, Nurliyana, MY, Chow, MJ, and Go, WZ. Reducing ash related operation problems of fast growing timber species and oil palm biomass for combustion applications using leaching techniques. *Energy*, 2015; 90: 622-630.
- [29] Idris, SS, Rahman, NA, and Ismail, K. Combustion characteristics of Malaysian oil palm biomass, sub-bituminous coal and their respective blends via thermogravimetric analysis (TGA). *Bioresource Technology*, 2012; 123: 581-591.
- [30] Slopicka, K, Bartocci, P, and Fantozzi, F. Thermogravimetric analysis and kinetic study of poplar wood pyrolysis. *Applied Energy*, 2012; 97: 491-497.
- [31] Açikalın, K. Thermogravimetric analysis of walnut shell as pyrolysis feedstock. *Journal of Thermal Analysis and Calorimetry*, 2011; 105(1): 145-150.
- [32] Maia, AAD and de Morais, LC. Kinetic parameters of red pepper waste as biomass to solid biofuel. *Bioresource Technology*, 2016; 204: 157-163.
- [33] Yang, H, Yan, R, Chen, H, Lee, DH, Liang, DT, and Zheng, C. Pyrolysis of palm oil wastes for enhanced production of hydrogen rich gases. *Fuel Processing Technology*, 2006; 87(10): 935-942.
- [34] Vassilev, SV, Baxter, D, Andersen, LK, and Vassileva, CG. An overview of the Chemical Composition of Biomass. *Fuel*, 2010; 89(5): 913-933.
- [35] Basu, P. *Biomass Gasification and Pyrolysis: Practical Design and Theory*. 2010.
- [36] Vassilev, SV, Vassileva, CG, and Vassilev, VS. Advantages and Disadvantages of Composition and Properties of Biomass in comparison with Coal: An overview. *Fuel*, 2015; 158: 330-350.
- [37] Miura, K and Maki, T. A Simple Method for Estimating  $f(E)$  and  $k_0(E)$  in the Distributed Activation Energy Model. *Energy & Fuels*, 1998; 12(5): 864-869.
- [38] Zsako, J. The kinetic compensation effect. *Journal of Thermal Analysis and Calorimetry*, 1976; 9(1): 101-108.
- [39] Turmanova, SC, Genieva, S, Dimitrova, A, and Vlaev, L. Non-isothermal degradation kinetics of filled with rice husk ash polypropylene composites. *Express Polymer Letters*, 2008; 2(2): 133-146.
- [40] Kim, YS, Kim, YS, and Kim, SH. Investigation of thermodynamic parameters in the thermal decomposition of plastic waste— waste lube oil compounds. *Environmental Science & Technology*, 2010; 44(13): 5313-5317.
- [41] Sheng, J, Ji, D, Yu, F, Cui, L, Zeng, Q, Ai, N, and Ji, J. Influence of chemical treatment on rice straw pyrolysis by TG-FTIR. *IERI Procedia*, 2014; 8: 30-34.

*To whom correspondence should be addressed: Dr. Bemgba B. Nyakuma, School of Chemical and Energy Engineering, Faculty of Engineering, Universiti Teknologi Malaysia, 81310 Skudai, Johor, Malaysia,  
E-mail: [bbnyax1@gmail.com](mailto:bbnyax1@gmail.com)*